Effect of Coefficient of Restitution on Thermodynamic Properties --- a 2D Simulation

Ziyao Xiong

***Abstract*—This report investigates the thermodynamic properties of a 2D multi-ball system under different coefficients of restitution (CoR). By analyzing key metrics such as pressure, temperature, kinetic energy, and momentum over time, we calculated the kinetic energy and temperature decay constant for CoR values of 0.8 and 0.9 to be 0.12 ± 0.01 and 0.077 ± 0.012, respectively, which are both within 5% range of theoretical values. Pressure decay constants is calculated to be 0.056 ± 0.013 and 0.035±0.014, which also align with theoretical prediction. We also concluded that the divergence between simulated data and ideal gas law prediction gets larger when CoR increases.**

I. Introduction

THE coefficient of restitution (CoR) is a measure of the elasticity of collisions between two bodies. In the context of gas dynamics, particularly non-ideal gases, the behavior of particles during collisions significantly impacts the macroscopic properties of the system [1]. This study aims to investigate the effect of varying CoR in a 2D thermosnooker simulation, providing insights into the relationship between energy dissipation and system thermodynamics and contributing to a deeper understanding of non-ideal gas dynamics in a confined environment.

II. Theory and Algorithm

A. Time to collision method

The simulation relies on accurately determining the time to collision between balls and between a ball and the container, followed by updating their velocities post-collision. Equation (1) is used to solve the time that next collision would occur:

$$[\mathbf{r}\cdot\mathbf{r}+2(\mathbf{r}\cdot\mathbf{v})\delta t+(\mathbf{v}\cdot\mathbf{v})(\delta t)^2-R^2=0], \quad (1)$$

where **r** and **v** are the relative position and relative velocity of two ball objects. *R* is the sum of the radii for ball-ball collisions or the difference in radius between the ball and the container for ball-container collisions. We select the smallest non-complex positive solution as the next collision time. Occasionally, no solution exists, but due to the finite representation of real numbers in computers [2], a positive solution may be returned, leading to incorrect ball movements, such as overlapping or escaping from the container. These are floating-point errors. To address this, we introduced a small tolerance level. If the computed time to collision is less than 10^{-6} seconds, it is considered zero.

B. Collide method in multi-ball simulation

In a collision between two balls, the coefficient of restitution (CoR) is used to determine the post-collision velocities. The CoR is defined as the ratio of the relative speed after collision to the relative speed before collision along the line of impact. Mathematically, this is expressed as:

$$\mathrm{CoR}=\frac{\text{relative speed after collision}}{\text{relative speed before collision}}. \quad (2)$$

CoR < 1 indicates a loss of kinetic energy in the system; the smaller the CoR, the greater the loss of kinetic energy.

In collisions of two objects, CoR affects only the normal components, while the tangential components remain unchanged. The normal vector **n** is a unit vector along the line of impact, and the tangential vector **t** is a unit vector perpendicular to the normal vector in the collision plane. The initial velocities of each particle are decomposed into their normal and tangential components by taking the dot product with **n** and **t**. Given initial velocities $\mathbf{v_{1n}}$ and $\mathbf{v_{2n}}$ in normal direction and $\mathbf{v_{1t}}$ and $\mathbf{v_{2t}}$ in tangential direction of two colliding balls with masses *m1* and *m2*, the velocities after collision in the normal direction, $\mathbf{v'_{1n}}$ and $\mathbf{v'_{2n}}$, are calculated using momentum conservation law and the definition of CoR:

$$\mathbf{v}'_{1\mathrm{n}}=\mathbf{v}_{1\mathrm{n}}+\frac{m_2}{m_1+m_2}(1+\mathrm{CoR})(\mathbf{v}_{2\mathrm{n}}-\mathbf{v}_{1\mathrm{n}}), \quad (3)$$

$$\mathbf{v}'_{2\mathrm{n}}=\mathbf{v}_{2\mathrm{n}}+\frac{m_1}{m_1+m_2}(1+\mathrm{CoR})(\mathbf{v}_{1\mathrm{n}}-\mathbf{v}_{2\mathrm{n}}). \quad (4)$$

Finally, the new velocities $\mathbf{v'_1}$ and $\mathbf{v'_2}$ of the particles are recombined by adding the normal and tangential components:

$$\mathbf{v}'_1=\mathbf{v}'_{1\mathrm{n}}\cdot\mathbf{n}+\mathbf{v}_{1\mathrm{t}}\cdot\boldsymbol{t},\ \mathbf{v}'_2=\mathbf{v}'_{2\mathrm{n}}\cdot\mathbf{n}+\mathbf{v}_{2\mathrm{t}}\cdot\boldsymbol{t}. \quad (5)$$

In a multi-ball simulation, the system comprises multiple balls interacting with each other and the container boundaries. The container is defined by a specified radius and a massive mass (10^7 kg) to ensure its position remains generally unchanged. The balls are initialized with properties such as radius, speed, mass, and positions generated in concentric rings. Each ball has an input speed and a randomized initial direction. Collision detection methods first check all possible pairs of balls for collisions, then check each ball for collisions with the container. The smallest positive time to collision is selected as the next collision event, and all balls are moved to their positions at that time. The colliding objects then collide, updating their velocities based on Equations (3), (4), and (5).

C. Thermodynamic properties

In each collision, the fraction of kinetic energy retained after a collision is proportional to CoR^{2n}, where *n* is the number of collisions. Alternatively, we can express it as:

$$KE(t)=KE(0)\cdot \mathrm{e}^{-\mathrm{kt}},\ k=\frac{-2\ln(CoR)}{\tau}, \quad (6)$$

where k represents the decay constant and τ represents characteristic time scale related to the average time between collisions [3]. τ can be calculated using:

$$\tau=\frac{\lambda}{\langle v\rangle},\ \lambda=\frac{1}{\sqrt{2}\,\mathrm{n}\,\sigma}, \quad (7)$$

where $\langle v\rangle$ represents the average speed of particles and λ is the average distance a particle travels between collisions called mean free path. λ can be calculated using the number density of particles *n* and the effective collision cross-section σ. In 3D, σ can be estimated by $4\pi\mathrm{r}^2$ [4], but in 2D we convert it into $2\pi\mathrm{r}$, where r is the radius of particles.

The equipartition theorem relates the temperature to the average kinetic energy of the particles. For a system of balls in 2D, n=2, the temperature *T* can be calculated using:

$$T=\frac{2\langle KE\rangle}{nk_B}=\frac{\langle KE\rangle}{k_B}, \quad (8)$$

where $\langle KE\rangle$ is the average kinetic energy. Since temperature is directly proportional to kinetic energy, it decays at the same rate as kinetic energy.

Due to the loss of kinetic energy, particles gradually hit the walls slower and with smaller force. Thus, pressure also decays over time. Since it is proportional to the force exerted on the container, the fraction of pressure retained after each collision is proportional to CoR^{n} rather than CoR^{2n}.

Consequently, the pressure P decays one time slower than kinetic energy and temperature. We can express it as:

$$\mathrm{P}(t) = \mathrm{P}(0) \cdot \mathrm{e}^{-\frac{\mathrm{kt}}{2}},\ k = \frac{-2\ln(CoR)}{\tau}. \quad (9)$$

If CoR=1, the temperature and pressure of the system can be calculated by ideal gas law, given by:

$$\mathrm{PV} = \mathrm{Nk_B T}, \quad (10)$$

where N is the number of particles, k_B is the Boltzmann constant, V is the volume. It assumes particles collide elastically; therefore, we expect to see a divergence of the simulated data with CoR<1 from the ideal gas law.

D. Units

In our 2D simulation, we must adjust the equations and units. Volume is the 2D area of the container, so number density is in m^{-2}. Surface area is represented by the perimeter of the container, thus pressure is in Pa·m. Other quantities remain the same as in 3D.

III. Results and Discussion

A. Momentum, kinetic energy, and temperature

The momentum of the ball-container system is calculated by summing up the mv_x and mv_y of the balls and the container after each collision. We ran 500 collisions for 37 balls with a radius of 1 m, mass of 1 kg, and initial speed of 10 m/s in a container with a radius of 10 m and mass of 10^7 kg. In the simulated animation, these parameters performed well, demonstrating reasonable movements and correct mechanics, thus we will use them for the following analysis unless stated otherwise. Fig.4 and Fig.5 show the momentum ratio to initial momentum over time in the x and y directions, respectively. Regardless of whether the CoR is 0.8, 0.9, or 1.0, the momentum ratio stabilizes well at 1, consistent with the conservation of momentum.

As shown in Fig. 3, when CoR = 1, the kinetic energy conserves as expected. However, when CoR = 0.8 and 0.9, the kinetic energy decays exponentially, with CoR = 0.8 decaying faster due to greater kinetic energy loss. This aligns with our prediction in Equation (6). Thus, we can fit the curves with Equation (6), as shown in Fig.6 and Fig.7. The best-fit decay constant, k, has values of 0.116 ± 0.001 and 0.0775 ± 0.0006 in these two particular simulations. Considering the randomness of the simulation, we ran the simulations five times and calculated the average k to be 0.117±0.01 for CoR=0.8 and 0.077±0.012 for CoR=0.9, with uncertainties derived from the range between the maximum and minimum possible k values.

Additionally, we calculated k using theoretical values derived from the mean free path and average speed. Utilizing Equations (6) and (7), the effective collision cross-section (σ) was determined to be 0.401 m, the number density (n) was 0.118 particles/m^2, and the mean free path (λ) was 15.010 m. The average speed over 500 collisions was measured in the simulations as 4.23±0.37m/s and 5.43±0.42m/s for CoR values of 0.8 and 0.9, respectively. From these values, we calculated the characteristic time scale (τ) to be 3.55±0.65s and 2.76±0.89s. These results align with expectations since a smaller CoR correlates with greater kinetic energy loss, resulting in a longer time to handle collisions. Consequently, the theoretical k values were determined to be 0.126±0.005 and 0.076±0.011, which correspond closely with the k values obtained from the curve fitting.

However, a divergence between the simulated data and the fitted curve is observed in the graphs. This discrepancy is attributed to the limitation of our model, where τ is treated as a constant despite its actual dependence on time due to changing average speeds. Nonetheless, our assumption of a constant average speed and τ is validated by the high accuracy of the resulting k values. Therefore, we accept this assumption for our analysis.

We expect temperature to decay at the same rate as kinetic energy. As illustrated in Fig.8 and Fig.9, the temperature ratio exhibits the same best-fit decay constant k as that of KE, validating the accuracy of the simulation results.

B. Pressure

The evolution of pressure over time for 500 collisions is shown in Fig.10. For all CoRs (0.8, 0.9, 1.0), the pressure initially experiences a rapid and unstable increase before stabilizing. This initial instability occurs because there are no initial collisions with the container; after a short period, a stable number of collisions with the container is established. For CoR = 1.0, the pressure stabilizes at approximately 17 Pa·m. For CoR values of 0.8 and 0.9, the pressure decays exponentially, aligning with our expectations. To avoid the initial unstable phase, we allowed 50 collisions to occur before fitting the pressure ratio with Equation (9). The choice of 50 collisions avoids the initial unstable range and ensures data quality by preventing excessive pressure decay and the associated high percentage uncertainty. As shown in Fig.11 and Fig.12, the mean k over five simulations were determined to be 0.056 ± 0.013 and 0.036 ± 0.014 for CoR values of 0.8 and 0.9, respectively. These values are expected to be half of the k values for kinetic energy and temperature. Indeed, doubling these values yields 0.112 ± 0.026 and 0.072 ± 0.028, which are within 5% of the k values for kinetic energy and temperature, indicating the correctness of our model.

C. Comparation with ideal gas law

Figs. 13, 14, and 15 show the PT, PV, and PN plots with simulation data and ideal gas law (IGL) predictions for different ball radii when CoR = 1. The data reveal that smaller radii result in better fits to the IGL. This trend is also evident in Fig. 16, where temperatures calculated from the equipartition theorem (Equation (8)) align with those from the IGL (Equation (10)) for smaller radii. To investigate the effect of CoR on the divergence from the IGL, we eliminated the radius effect by setting the radius to 0.001 m. The simulated pressure/IGL predicted pressure versus temperature is shown in Fig. 17. As expected, for CoR = 1, the scatter points are concentrated around y=1, indicating good consistency between the IGL and simulation. However, for CoR = 0.8 and 0.9, the points are concentrated at higher y values, indicating greater disagreement with the IGL as CoR decreases. Also, points with smaller CoR are positioned at lower temperatures, consistent with theoretical expectations.

IV. Conclusion

Our simulation successfully obtained decay constants for kinetic energy and pressure that align well with theoretical predictions, and the data patterns in the graphs are correct. However, several improvements can be made in this investigation. We only studied three CoR values; expanding the range would provide a more comprehensive picture of its effects. We also ignored the time dependence of τ; although treating it as a constant is reasonable, it would be better to rigorously consider its time dependence. Additionally, due to the inherent randomness in each simulation, performing more simulations would better account for random errors in the investigation of each property.

REFERENCES

[1] R. Clausius, "On the Motive Power of Heat, and on the Laws which can be deduced from it for the Theory of Heat," Poggendorff's Annalen der Physik, vol. LXXIX, 1850 (Dover Reprint). ISBN 978-0-486-59065-3.

[2] "Floating decimal point arithmetic control means for calculator: United States Patent 3037701," FreePatentsOnline.com, 1962-06-05. [Online]. Available: https://www.freepatentsonline.com/3037701.html. [Accessed: 21-Jan-2022].

[3] S. Chapman and T. G. Cowling, The Mathematical Theory of Non-Uniform Gases, 3rd ed., Cambridge, U.K.: Cambridge University Press, 1990, p. 88. ISBN: 0-521-40844-X.

[4] A. Savara, "Comment on 'Equilibrium Constants and Rate Constants for Adsorbates: Two-Dimensional (2D) Ideal Gas, 2D Ideal Lattice Gas, and Ideal Hindered Translator Models'," J. Phys. Chem. C, vol. 120, no. 36, pp. 20478–20480, Aug. 2016. [Online]. Available: https://doi.org/10.1021/acs.jpcc.6b07553. [Accessed: 15-Jun-2024].

LIST OF PLOTS

Unless stated otherwise, the following graphs are generated with 500 collisions for 37 balls with a radius of 1 m, mass of 1 kg, and initial speed of 10 m/s in a container with a radius of 10 m and mass of 10^7 kg.

Task 11:

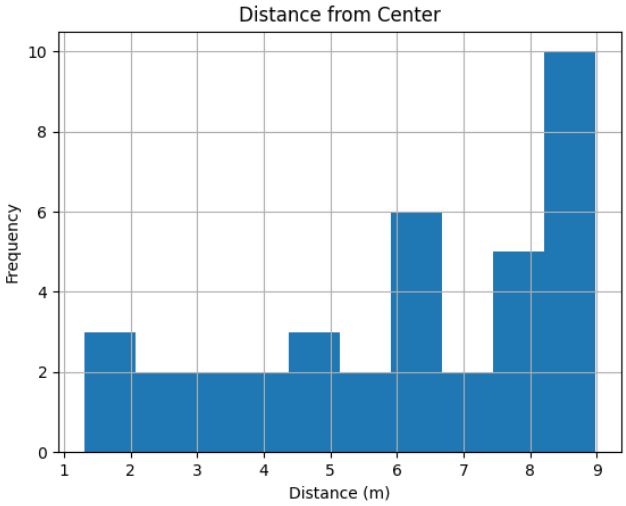

Fig.1. Histogram of balls' distances to the center of container. The largest distance is 9, indicating no balls are escaping from the container.

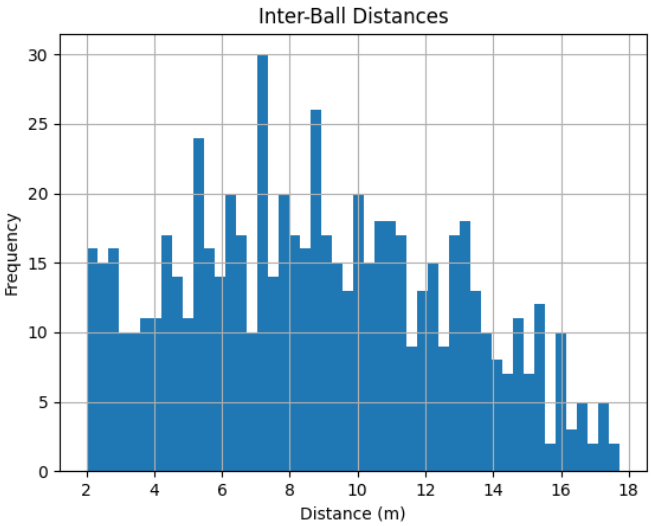

Fig.2. Histogram of balls' distances to each other. The smallest distance is 2, indicating no balls are overlapping.

Task12:

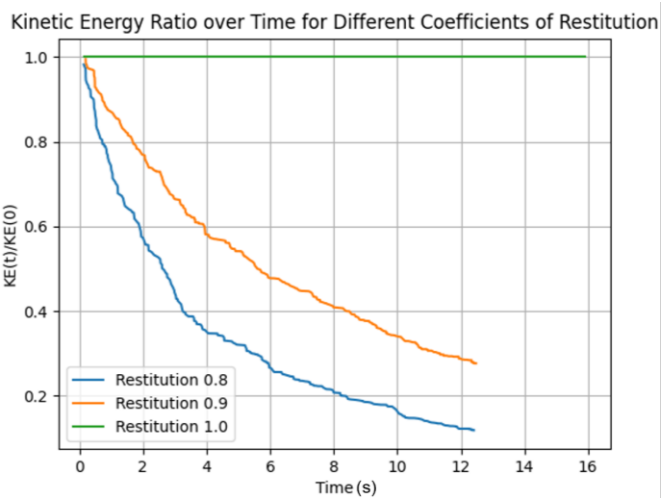

Fig.3. Evolution of the ratio of kinetic energy of the ball-container system to initial kinetic energy over 500 collisions. Kinetic energy is conserved when CoR = 1 and decreases exponentially when CoR < 1.

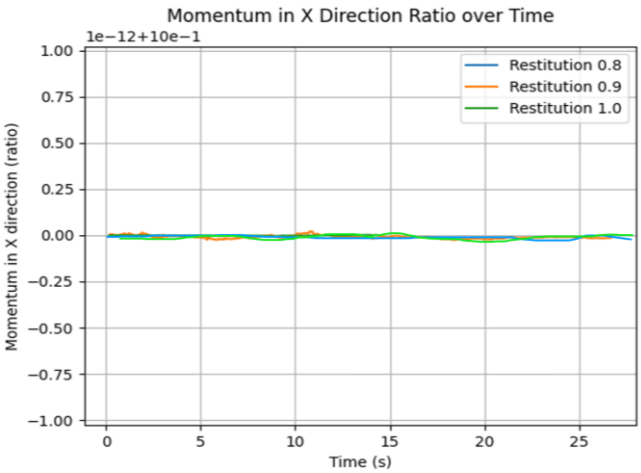

Fig.4. Evolution of the ratio of momentum of the ball-container system to initial momentum in the x direction. All CoR values present a constant straight line at 1, indicating conservation of momentum in the x direction. The small fluctuation can be explained by floating-point errors.

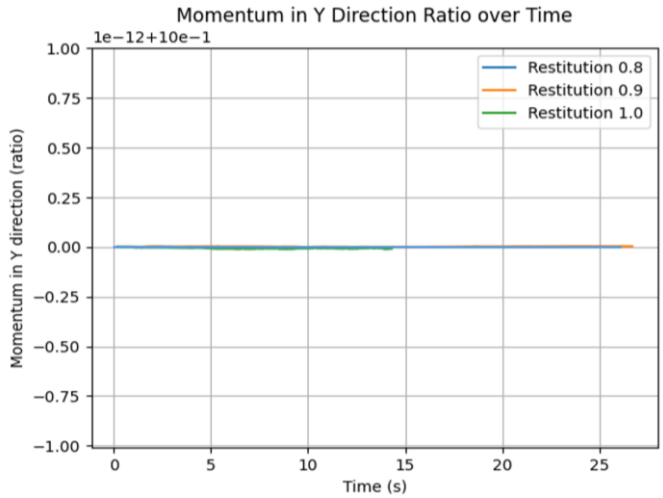

Fig.5. Evolution of the ratio of momentum of the ball-container system to initial momentum in the y direction. All CoR values present a constant straight line at 1, indicating conservation of momentum in the y direction. The small fluctuation can be explained by floating-point errors.

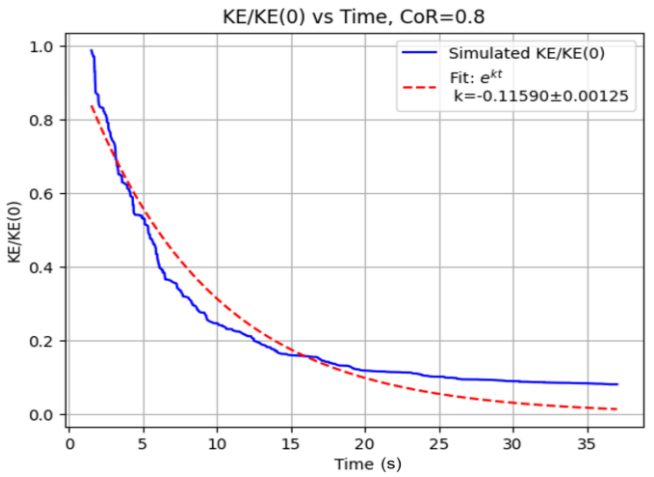

Fig.6. KE ratio for CoR = 0.8 fitted by an exponential decay curve. In this particular simulation, the decay constant k is best fitted as 0.116 ± 0.001. Four additional simulations were conducted, and the corresponding k values were generated. The average k value was then calculated.

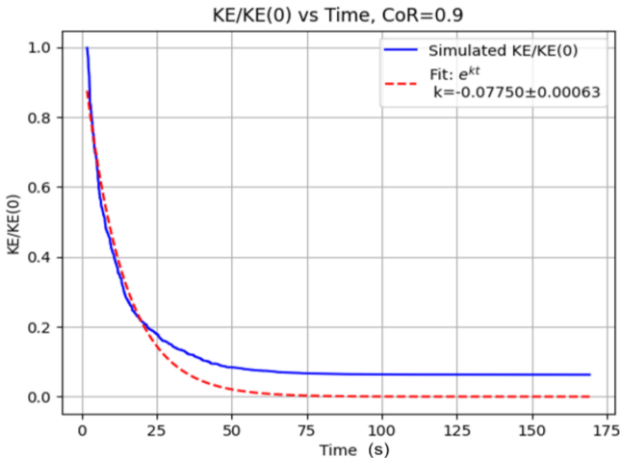

Fig.7. KE ratio for CoR = 0.9 fitted by an exponential decay curve. In this particular simulation, the decay constant k is best fitted as 0.0775 ± 0.0006. Four additional simulations were conducted, and the corresponding k values were generated. The average k value was then calculated.

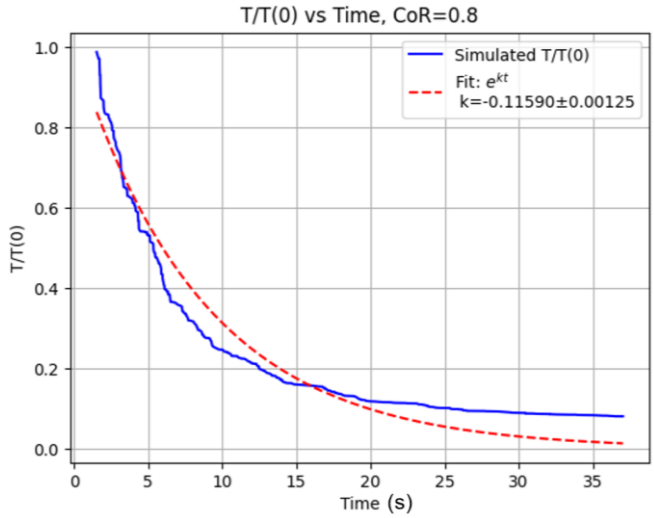

Fig.8. Temperature ratio for CoR = 0.8 fitted by an exponential decay curve. In this particular simulation, the decay constant k is best fitted as 0.116 ± 0.001, which is same as that of kinetic energy for the same CoR.

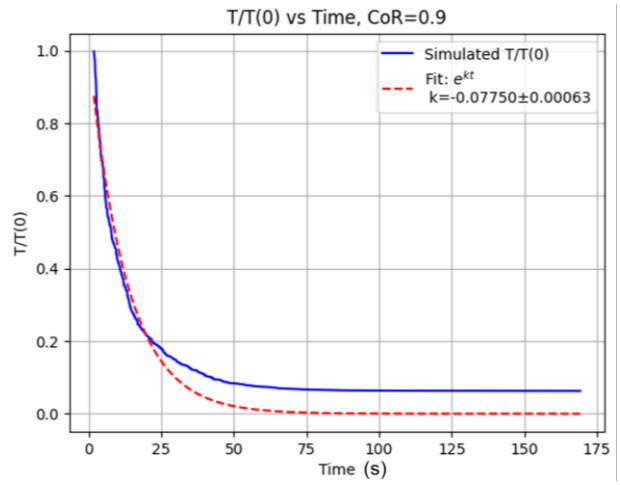

Fig.9. Temperature ratio for CoR = 0.9 fitted by an exponential decay curve. In this particular simulation, the decay constant k is best fitted as 0.0775 ± 0.0006, which is same as that of kinetic energy for the same CoR.

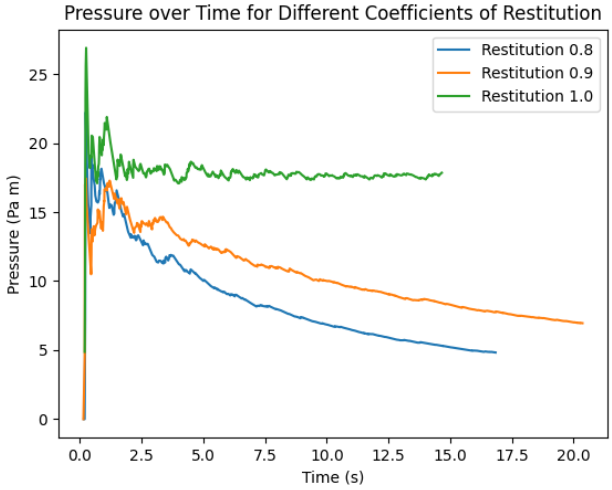

Fig.10. Pressure evolution over time during 500 collisions for different CoR values. All curves exhibit an initial unstable increase, followed by a stable trend. For CoR = 1, the pressure remains approximately constant at 17 Pa·m, while for CoR = 0.8 and 0.9, the pressure decays exponentially, with CoR = 0.8 decaying faster than CoR = 0.9.

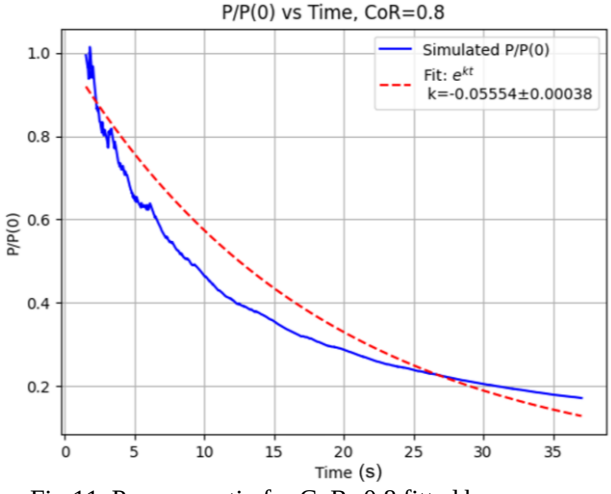

Fig.11. Pressure ratio for CoR=0.8 fitted by an exponential decay curve. In this particular simulation, the decay constant k is best fitted as 0.0555 ± 0.0004. Four additional simulations were conducted, and the corresponding k values were generated. The average k value was then calculated.

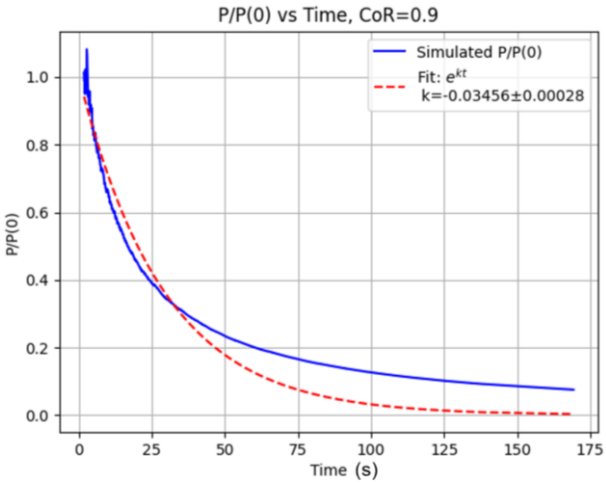

Fig.12. Pressure ratio for CoR=0.9 fitted by an exponential decay curve. In this particular simulation, the decay constant k is best fitted as 0.0346 ± 0.0003. Four additional simulations were conducted, and the corresponding k values were generated. The average k value was then calculated.

Task 13:

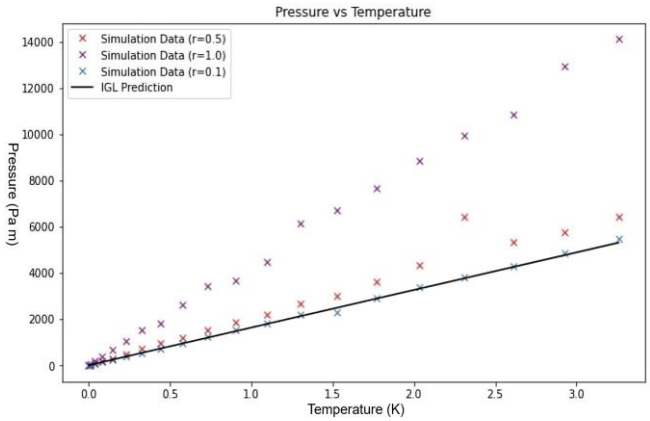

Fig.13. Comparison of simulated data and IGL prediction of pressure over temperature for different ball radii. Temperature is altered by changing the initial speed of the balls. Pressure is calculated by *F/A* (momentum/At), and IGL pressure is calculated by Nk_BT/V. When r=0.1, the IGL and simulation nearly overlap, indicating a good approximation. As the radius increases, the IGL prediction worsens.

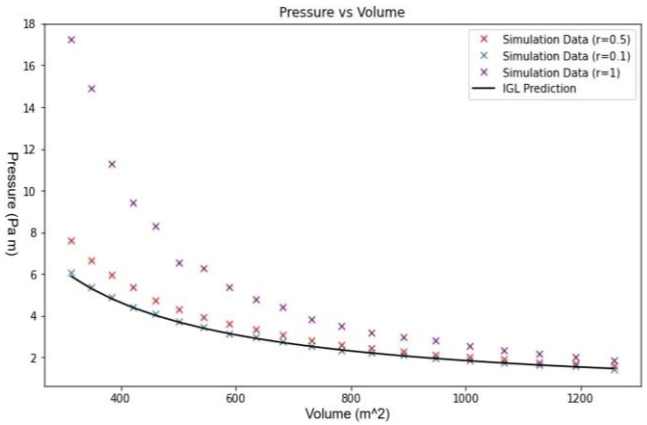

Fig.14. Comparison of simulated data and IGL prediction of pressure over volume for different ball radii. Volume is altered by changing the radius of the container. Pressure is calculated by *F/A* (momentum/At), and IGL pressure is calculated by Nk_BT/V. As the radius increases, the IGL prediction worsens.

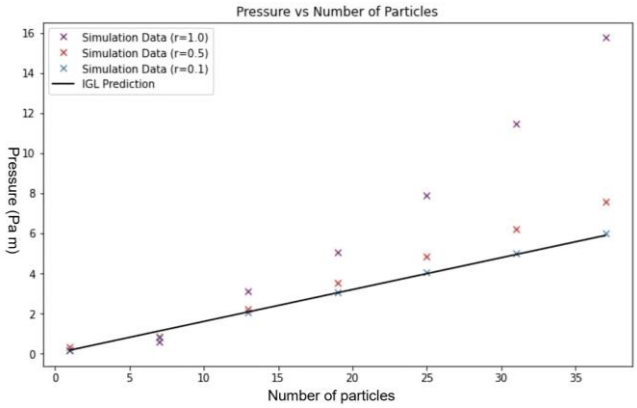

Fig.15. Comparison of simulated data and IGL prediction of pressure over number of particles for different ball radii. N is altered by changing the number of rings during initialization of positions of balls. Pressure is calculated by *F/A* (momentum/At), and IGL pressure is calculated by Nk_BT/V. As the radius increases, the IGL prediction worsens.

Task 14:

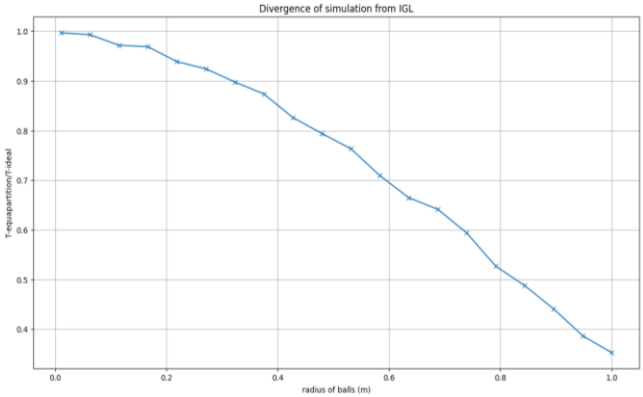

Fig.16. The ratio of temperature calculated from the equipartition theorem to temperature predicted from the IGL ($T=PV/Nk_B$) as a function of ball radius. Smaller radii result in ratios closer to one, indicating better consistency between the two temperatures. As the radius increases, the accuracy of the IGL prediction decreases.

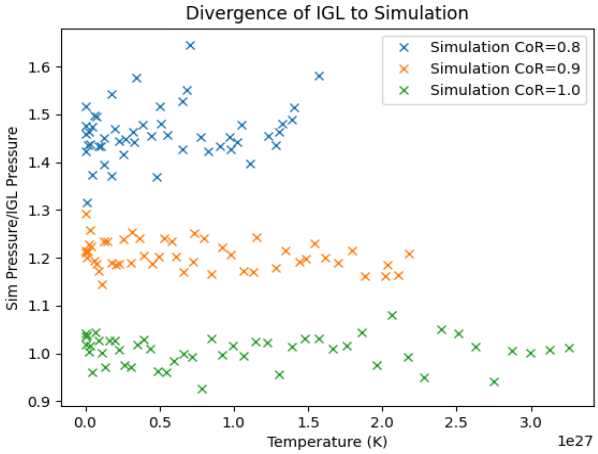

Fig.17. Comparison of the effect of CoR on divergence from the IGL. The ratio of simulated pressure to IGL predicted pressure over temperature is plotted. The ball radius is set to 0.01, so when CoR = 1, the simulation data/IGL prediction ratio equals 1, indicating good consistency. As CoR decreases, the simulated pressure becomes larger than the IGL prediction, and the accuracy of the IGL prediction decreases. Higher CoR values correspond to higher overall temperature patterns, indicating greater kinetic energy.

Task 15:

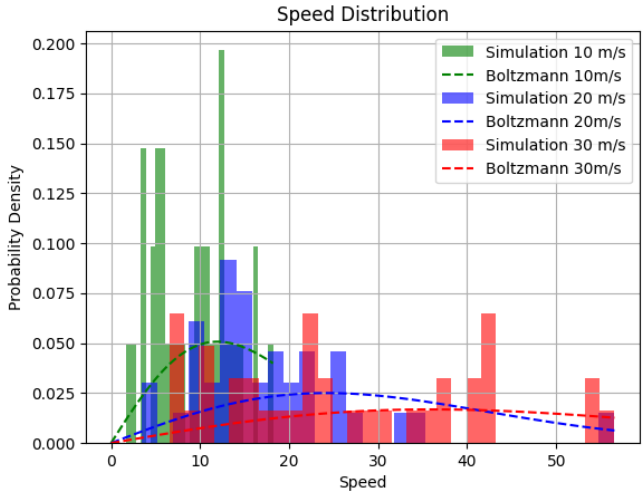

Fig.18. Speed distribution of balls in the simulation compared to Maxwell-Boltzmann distributions. The histograms represent the simulated speed distributions for initial speeds of 10m/s, 20m/s, and 30m/s. The corresponding Maxwell-Boltzmann distribution curves are overlaid. The probability density on the y-axis indicates the likelihood of speeds observed in the simulation. The simulation data and the Maxwell-Boltzmann distributions generally agrees with each other.